ANNALI DI GEOFISICA, VOL. XXXVII, N. 6, December 1994

Slip heterogeneity, body-wave spectra, and directivity of earthquake ruptures

Pascal Bernard and André Herrero
Département de Sismologie, I.P.G.P., Paris, France

Abstract
We present a broadband kinematic model based on a self-similar k-square distribution of the coseismic slip, with an instantaneous rise-time and a constant rupture velocity. The phase of the slip spectrum at high wave number is random. This model generates an ω-squared body-wave radiation, and a particular directivity factor C_d^2 scaling the amplitude of the body-wave spectra, where C_d is the standard directivity factor. Considering the source models with a propagating pulse and a finite rise-time, we assume that within the slipping band, the rupture has some random character, with small scale rupture in various directions. With such a model, the pulse cannot be resolved, and the directivity factor is still C_d^2 at low frequency; at periods shorter than the rise-time, however, the directivity effect drops to much smaller rms values. This frequency dependent directivity effect, which is expected to be the strongest for sites located in the direction of rupture, was evidenced for the Landers 1992 earthquake, leading to a 2 to 3 s rise-time of the slip pulse. This kinematic model can be used with more refined theoretical Green's functions, including near-field terms and surface waves, or with empirical Green's functions, for generating realistic broadband records in the vicinity of moderate to large earthquakes, in a frequency range relevant for engineering applications (0 Hz to about 20 Hz).

Key words *fault slip – seismic rupture – slip heterogeneity – directivity effect – kinematic rupture – stochastic model – isochrone – synthetic accelerogram – rise-time – body-wave spectrum*

1. Introduction

The spectral characteristics of the earthquake source radiation, evidenced by teleseismic records at frequencies up to 1 Hz, as well as by the near-source records for higher frequencies, reflect both the complexity of the rupture process and of the wave propagation. The dominant spectral effect of the latter is now quite well modelled, taking into account the whole path or near-surface attenuation, and near-surface specific resonances. Standard spectral models of radiation, such as the ω-squared model (Aki, 1967), or other spectral laws (Hartzell and Heaton, 1985: $\omega^{-1.5}$; Boatwright and Choy, 1992: ω^{-1} for intermediate frequencies), have implicitly corrected for, or avoided these propagation effects, and are assumed to describe the source spectral characteristics. These spectral laws must then reflect some scaling law between the kinematic parameters of the rupture, and hence between some parameters controlling the rupture dynamics.

The aim of the present paper was to determine the effect of the spatial distribution of the coseismic slip on the radiated spectrum, assuming a constant rupture velocity, and to discuss its consequences in terms of ground motion amplitudes, spectra and directivity effects.

2. Space-time slip singularities generating ω^2 models

The propagation of a uniform dislocation on a fault at a constant rupture velocity, with a rise-time $\tau = 0$, is well known for generating

an ω-squared bodywave displacement spectrum. The classical Haskell model, assigning a constant and finite rise-time τ for a uniform dislocation, thus generates an ω^2 decay for frequencies larger than the corner frequency and smaller than $1/\tau$ – as for an instantaneous slip –, and an ω^3 spectral decay for higher frequencies, due to the time filtering. The origin of this ω^2 decay is the singularity of the far-field displacement due to the interaction of the isochrones with the four corners of the rectangular fault (*e.g.*, Bernard and Madariaga, 1984), as sketched in fig. 1a-d. The radiated far-field displacement has indeed a trapezoidal shape, thus presenting four second-order singularities (discontinuities in the slope), leading to the ω^2 spectral decay. Taking the second derivative of this function in order to synthetize the ground acceleration, four delta functions are obtained at the four critical times, and zero elsewhere: the resulting acceleration peaks are thus completely unrealistic. In other words, all the energy of the ground motion spectrum would be distributed in a non-stationary way. Furthermore, this model may present a pathological geometry when the isochrones are parallel to one edge, generating a box-car shape displacement associated with an ω^{-1} spectral decay, thus with even stronger singularities. These can be reduced at high frequencies by assuming a finite rise-time, resulting in a still unrealistic trapezoidal displacement.

Even for more realistic quasi-dynamic source models, with inverse square root spatial singularities of the slip velocity and barriers associated with jumps in slip or in rupture ve-

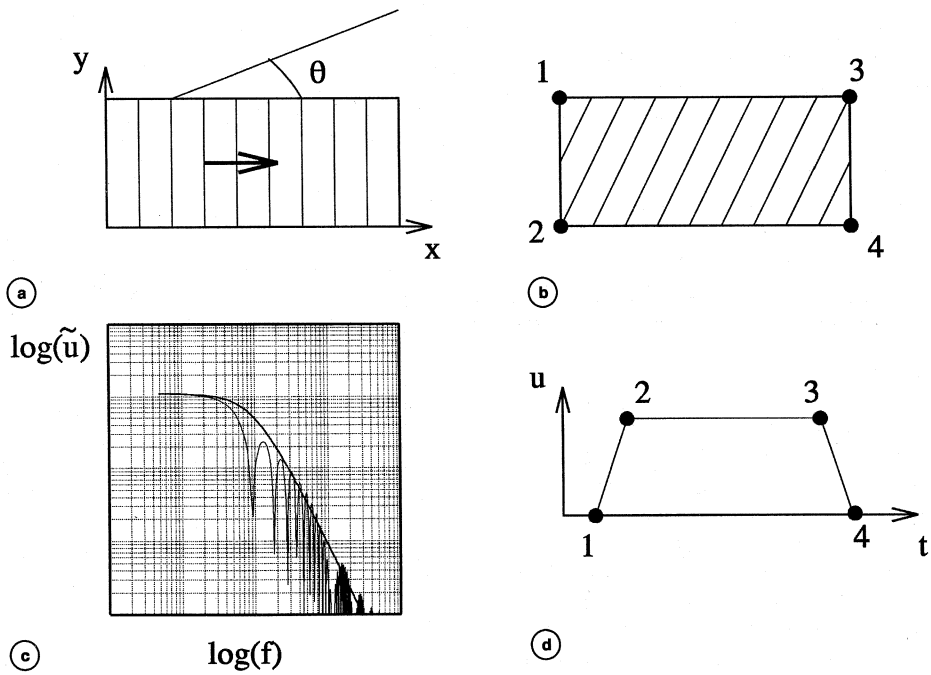

Fig. 1a-d. Spectrum for Haskell's kinematic rupture model. a) Propagation of the rupture front at constant rupture velocity; b) corresponding isochrones for a site in the azimuth θ; c) corresponding far-field displacement spectrum, decaying in f^{-2}; d) corresponding far-field displacement wave-form, whose singularities come from the interaction of the isochrone with the four corners of the rectangular fault (labelled 1, 2, 3, 4). Discontinuities in the slope of the time function generates the f^{-2} decay of the spectrum.

locity, Bernard and Madariaga (1984) showed that the high frequency radiation came from a limited number of points, where the isochrone length presents some singular time variations («stopping» phases). Note that starting phases have weaker singularities than stopping phases, for two reasons: first, their associated isochrone length increases linearly with time from the nucleation point, instead of presenting a square root singularity due to the local tangency between the isochrone and the barrier. Second, the slip velocity itself is less singular for the starting phase, as the slip is constrained by the size of the growing rupture. In total, body-wave spectra from stopping phases are expected to be ω times larger than those from starting phases.

Such kinematic models with singularities are, however, not satisfactory, because the origin of the dominant high frequency radiation for real earthquakes is observed to be more evenly – or randomly – distributed on the whole fault, and not concentrated at a few points (four points for a rectangular fault, two points for a circular source). The fact that strong ground motion acceleration peaks can be correctly estimated using the ω^2 model and by assuming a stochastic signal lasting the total rupture duration is clear evidence of the nearly stationary character of the accelerogram (Boore, 1986). Thus, models with a few strong singularities are clearly unsuitable if the recording site is at a distance of the order or smaller than the size of the ruptured area, because the predicted maximal amplitudes will be extremely large, with a very small duration, at the arrival times of the singularities, although the associated displacement spectrum may present the proper level and frequency decay.

It is worth noting here that most of the Empirical Green Function (EGF) methods used for simulating strong ground motions with the records of small earthquakes implicitly generate their ω^2 source spectra with a space-time distribution of subevent weights which present singularities similar to those associated with the instantaneous slip model with constant dislocation described above. This means that if the EGF was replaced by the impulsive numerical Green function of a homogeneous half space, the simulated acceleration record would present zero or very weak amplitude most of the time, except at the arrival time of the singularities, as explained above. If the EGF itself is quite impulsive, which may often be the case for near-source distances – under a few tens of kilometers – this concentration of the acceleration energy around the singularity arrival times will remain, and may lead to unacceptably high values for the peak accelerations.

3. The «k^2» model of coseismic slip

In order to avoid these difficulties, and to distribute the high frequency sources more evenly over the whole ruptured area, several authors have introduced kinematic models presenting some complexity in the slip distribution or in the rupture kinematics, simulating composite earthquakes (*e.g.*, Papageorgiou and Aki, 1983). However, these models produce very specific spectra, usually with an intermediate spectral slope in $1/\omega$ between the corner frequency of the total rupture and some higher frequency related to the size of the subevents, and are thus difficult to adapt for simulating the ω^2 radiation, or any other spectral behaviour.

We recently introduced a simple kinematic model of earthquake rupture which is able to generate a wide range of spectral shapes for the far-field radiation spectra, including the ω^2 model (Herrero and Bernard, 1994). The basic assumption is that the physical source of the far-field radiation is randomly distributed over the fault plane, and dominantly due to the spatial heterogeneity of the coseismic slip. We will limit the following discussion to the ω^2 radiating models.

Our first assumption is that the amplitude of the slip distribution, high passed at high wave numbers, does not depend on the size of the ruptured fault. This means that there is a «local» control of the slip heterogeneity at any scale, independent of heterogeneities at a larger scale. This leads to the following «k^2» model for the slip spectrum, for $k > 1/L$:

$$\Delta u_L(k) = C\, \Delta\sigma/\mu\; L/k^2$$

where L is the ruptured fault dimension, k the radial wave number, $\Delta\sigma$ the mean stress drop, μ the rigidity, and C an adimensional constant of the order of 1. The associated stress drop spectrum, for $k > 1/L$, is then approximated by

$$\Delta\sigma_L(k) = \Delta\sigma L/k .$$

This result was first given by Andrews (1981). Frankel (1991) deduced a similar power law decay in the case of a discrete, self-similar distribution of subevents on a fault plane. Other power laws have been proposed, such as $1/k^3$ (Hanks, 1979), and $1/k$ (Lomnitz-Adler and Lemus-Diaz, 1989). These spectral laws are sketched in fig. 2a-c. For exponents smaller than 2, the rms stress drop on the fault plane strongly diverges at high frequencies, which is not physically acceptable. On the other hand, Hanks' model gives a very smooth slip distribution at high wave numbers. The $1/k^2$ decay of the slip distribution implies a very weak divergence of the rms stress drop, which is physically acceptable. It may be interpreted as an approximately constant strain on the fault surface at all scales.

A numerical simulation of the slip distribution for a magnitude 6 earthquake is presented in fig. 3. The spectral amplitude is imposed by the scaling law described above, and the phase is random at any wave number, except for the very lowest terms, for which the phase is chosen in order to have a maximal slip near the center of the rectangular fault.

4. Source kinematics with a constant rupture velocity

We have now to define the kinematics of the rupture. We simply assume a constant rupture velocity, and a self-similar rise-time depending on the scale of the process. This means that the time necessary for completing the partial slip at a given wave number is proportional to the corresponding wavelength. In other words, subevents break in a time proportional to their size. The simplest way to achieve such a scale dependent rise-time is by using a dislocation model (instantaneous slip at the final value): in which case, the rupture front travels through a subarea with length $1/k$ in a time $1/kv$, where v is the rupture front velocity.

The far-field displacement $u(t)$ is well known to be the integral over the fault area of the slip velocity, scaled by distance and radia-

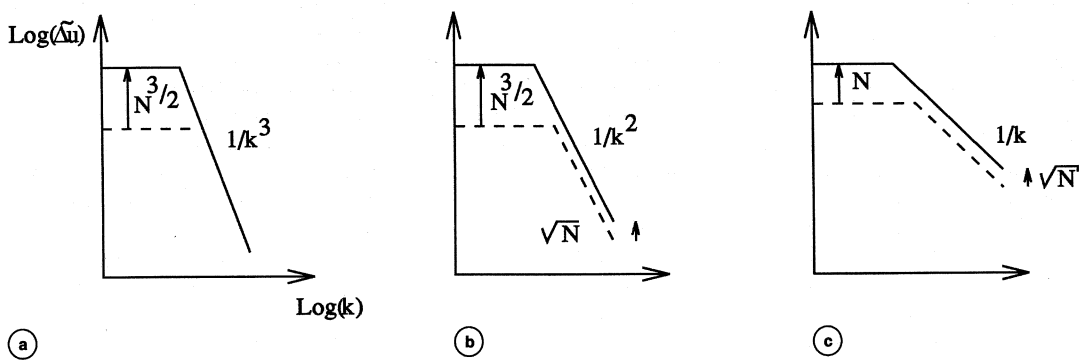

Fig. 2a-c. Spectral laws for the slip distribution on the fault. This summarizes the different slip distribution spectra that we infer from the results of: a) Hanks (1979); b) Andrews (1981), a particular solution of Frankel (1991) and the «k^2 model of this study; c) Lomnitz-Adler and Lemus-Diaz (1989). We consider two distributions on faults with characteristic lengths L_0 (solid line) and $L_1 = L_0 / 2$ (dashed line). N is the ratio of the areas ($N = L_0^2 / L_1^2$).

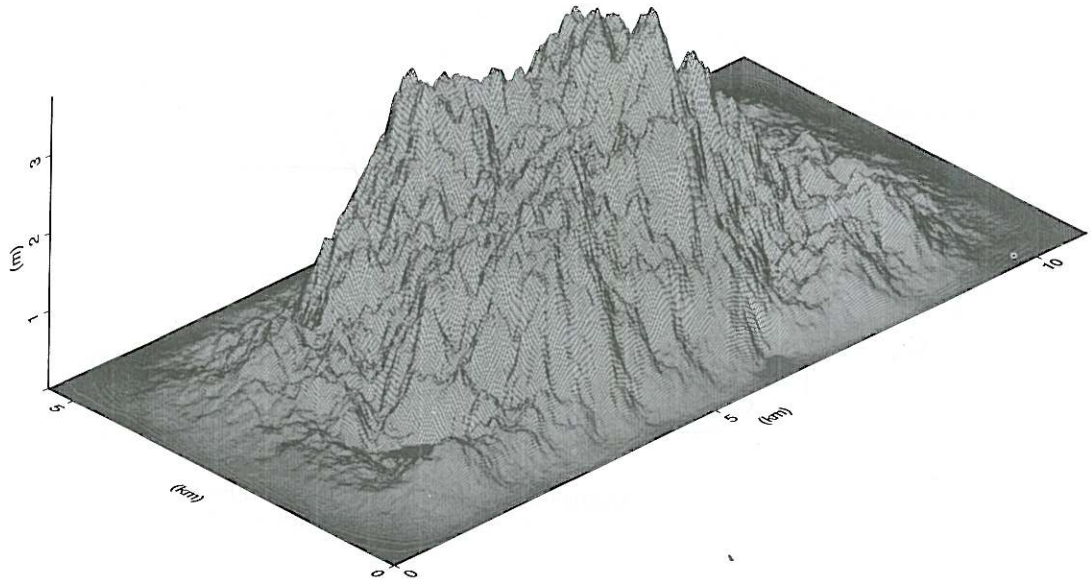

Fig. 3. k^2 model of the slip for a magnitude 6 earthquake. The k^2 model of the slip is scaled by a fault length $L = 10.8$ km, a stress drop $\Delta\sigma = 4$ MPa, a rigidity $\mu = 3.3\ 10^{10}$ Nm, and a coefficient $C = 1$. The slip is tapered at the edge of the fault, and the negative values are set to zero. The phase of the lowest wavenumbers is calculated in order to concentrate the slip near the center of the fault. At higher wavenumbers, the phase is random.

tion pattern, and delayed by the travel time. For an instantaneous slip and a propagation in the x-direction, the slip velocity is of the form $\delta(t - x/v)$. For a rectangular fault, with isochrones propagating in the x direction, it is then straightforward to obtain the relationship betweeen the far-field displacement spectrum $u(\omega)$ and the slip spectrum $\Delta u(k_x, k_y)$, as shown by Bernard (1987) and Herrero and Bernard (1994):

$$u(\omega) = F\ \Delta u(k_x = \omega/(C_d\, v),\ k_y = 0)$$

where the factor F includes radiation pattern and distance effect, and C_d is the classical directivity coefficient: $C_d = 1/(1 - v/c\ \cos\ \theta)$. The angle θ is the angle between the seismic ray and the direction normal to the isochrone, which coincides with the direction of the rupture in this simple case, and c is the body-wave velocity (P or S wave). Note that this formula exhibits the classical shift of the corner frequency by the factor C_d.

The k^2 model for the slip thus leads to the ω^2 model, with the assumptions above. In that case, the acceleration spectral level for frequencies larger than the corner frequency is proportional to $C_d{}^2$, as illustrated in fig. 4 and table I. This C_d^2 factor was also theoretically deduced by Joyner (1991) from ω^2 models.

We present here the simulation of the radiation of a magnitude 6 earthquake fault. The slip distribution used is that of fig. 3. The propagation terms are restricted to the far-field terms in an elastic half-space, with an attenuation characterized by $\kappa = 0.08$ (hard rock site). The site is located at 13 km from the fault plane. The accelerogram and its spectrum is presented in fig. 5. Both time and spectral amplitudes are in good agreement with statistical results (*e.g.*, Joyner and Boore, 1981).

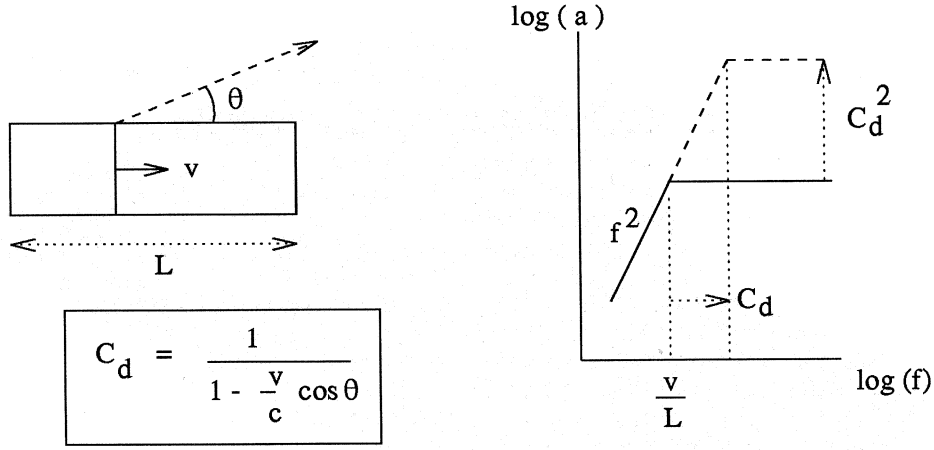

Fig. 4. Spectral effect of the directivity. The apparent corner frequency is multiplied by C_d, thus shifted towards higher frequencies when θ is smaller than 90°. The ω^2 model thus implies a shift of the acceleration spectral level by a factor C_d^2.

Table I. Squared directivity factor C_d^2.

v/β \ θ	0°	90°	180°
0.9	100	1	0.28
0.8	25	1	0.31
0.7	11	1	0.35

5. Rupture velocity and rise-time

Although the proposed kinematic model is realistic in terms of stress drop and coseismic slip distribution, the assumptions of a constant rupture velocity and an instantaneous slip do not seem satisfactory in terms of rupture dynamics. Let us discuss here these assumptions.

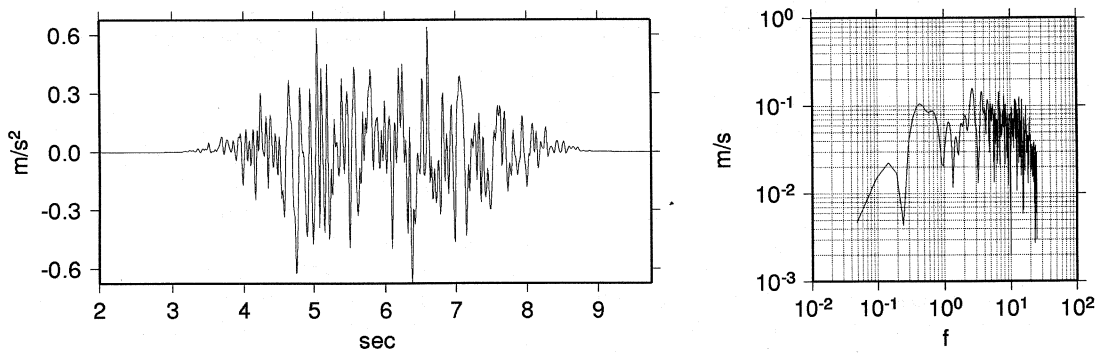

Fig. 5. Synthetic *S*-wave acceleration from the kinematic model. Direct *S*-wave acceleration and corresponding spectrum were simulated at a site 13 km away from the fault described in fig. 3 ($M = 6$). The peak acceleration value, about 0.6 m/s^2, the apparent source duration, about 5 s, and the spectral shape, with its clear corner frequency and flat acceleration at high frequencies, are characteristic for this distance and magnitude.

The hypothesis of a constant rupture velocity can be simply seen as a numerical trick for modeling the effects of the true space-time slip velocity variability, by using the effects of an ad-hoc final slip distribution associated with a smooth regular rupture front propagation. Therefore, the k^2 model can be seen as the upper limit of the slip spectra: very smooth slip distribution could be compensated by heterogeneous rupture velocity for generating the ω^{-2} radiation spectrum. The real process may lie between these two extreme models, the heterogeneities in slip and rupture velocity both being responsible for the radiation spectral decay. The analytical or numerical description of the rupture kinematics which would be required for modeling this process does not seem simple, and is beyond the scope of the present paper. For the practical purpose of simulating realistic high frequency waves, assuming a constant rupture velocity is simpler to handle and provides adequate results.

The second problem comes from the assumption of an instantaneous slip, which is clearly unphysical. A more standard slip history would require a constant rupture velocity during a finite rise-time T. This, however, would result in a low-pass filtering of the radiated waves. In the specific case of the k^2 model of slip, it would result in a change from an ω^2 decay to an ω^3 decay at frequencies higher than $1/T$. Let us first note that such an abrupt change in the radiation spectral laws is not evidenced in the data, which seem to rule out the constant slip velocity model: the true slip velocity has to be variable in time at any given slipping point on the fault. Andrews (1981) indeed showed that this function should decay as ω^2 and k^2 in the frequency-wave number domain in order to produce an ω^2 displacement in the far-field. This k and ω dependence implies that the variable slip velocity should present some space-time correlation in the volume limited by the two space-time surfaces defined by the rupture front and by the following «locking» front (or «healing» front) (fig. 6).

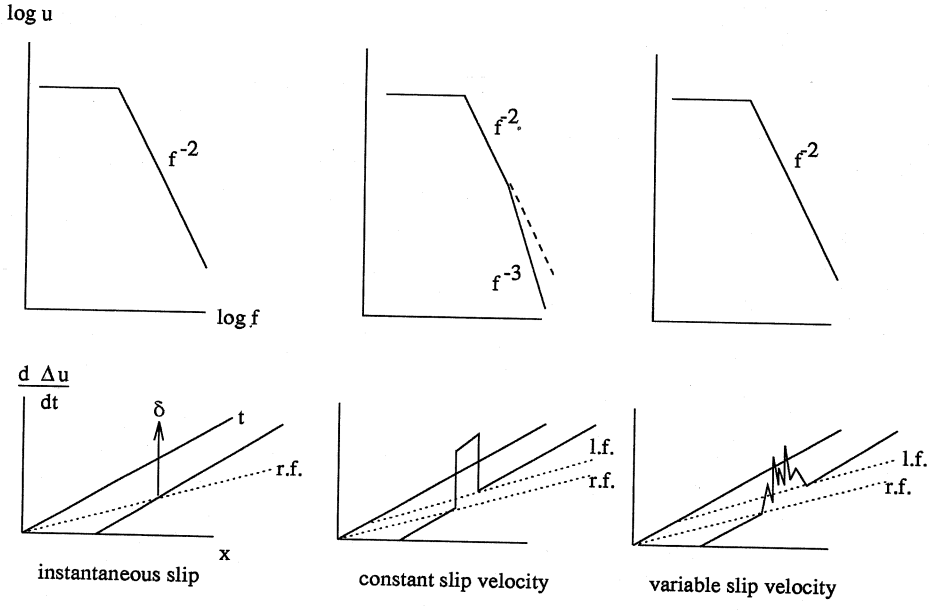

Fig. 6. Slip velocity function and body-wave spectra. Three slip velocity functions are considered (bottom), with the associated body-wave displacement spectra (top) deduced from a k^2 model of the slip. Label r.f. is for the rupture front; l.f. is for the locking front. Left: the instantaneous slip model considered in the present study, generating the ω^2. Center: the constant slip velocity model, resulting in a low-pass filtering of the spectra. Right: variable slip velocity in the slipping band characterized by a k^2 and ω^2 space-time correlation.

One could imagine that a number of small ruptures nucleate within the slipping band, at different scales up to the length of the slipping band itself, resulting in some very complicated space-time correlations of the slip velocity pulses. In our case, the space-time correlation is very particular, as the rupture band, which has a width vT, is degenerated into the rupture front line ($T = 0$).

For periods smaller than the rise-time, our assumption may thus be considered the simplest numerical approach for generating a slip velocity with the appropriate spectral decay above: indeed, our choice of an instantaneous slip leads to a $1/(k^2 + (\omega/v)^2)$ asymptotic behaviour for the slip velocity.

For periods longer than the rise-time, our approximation of an instantaneous slip remains acceptable. Note that according to recent models of self-healing pulses (see Heaton, 1990), this rise-time may not exceed a few seconds for large earthquakes, which means that our assumption would be justified for interpreting and modeling the observation of spectral decay for long periods down to a few seconds.

6. Frequency dependence of directivity effects

6.1. *A speculative model*

The specific space-time coherence of the slip velocity resulting from a constant rupture velocity and an instantaneous slip results in a particular directivity effect, which requires some discussion. Indeed, the theoretical C_d^2 directivity coefficient deduced from the model (see above) can reach the value of several tens up to 100 for S waves (taking $\theta = 0$ and $v/c = 0.9$). Such a directivity effect on the spectral level should appear also in the peak accelerations, with the same amplification: this is however not reported, an amplification factor of about 10 being the maximal effects observed for acceleration records at sites in the direction of the rupture propagation.

In order to reduce the directivity effect of our model at high frequencies, we propose that at periods smaller than a given period T_0, hence for wavelengths smaller than vT_0, the rupture becomes incoherent, being the sum of small scale rupture with random directions. The directivity coefficient would then be the quadratic sum of C_d^2 coefficients with variable θ corresponding to variable rupture directions on the fault plane for large k. For the most directive case ($\theta = 0$), this root mean square C_d^2 coefficient is about 1/4 of the classical C_d^2 value. This frequency dependence of the directivity at a given site is illustrated in fig. 7a. We suggest that this T_0 is of the order of the actual maximal rise-time on the fault plane: subevents which are smaller than the width of the radiating area at a given time may indeed have a rupture direction different from the main direction of the rupture propagation, as sketched in fig. 7b.

The length $L_0 = vT_0$ represents the size, in the direction of the rupture, of the slipping area, at a given time: it thus describes the average length of a propagating pulse. This length may be of the order of the source width, if it is controlled by the stopping phases coming from the source edge, as for the crack models. Alternatively, it may be much smaller if it is related to a «self-healing» pulse, as proposed by Heaton (1990). Our model may thus describe a wide variety of ruptures, provided that the pulse width does not changes too much during the main part of the rupture propagation.

6.2. *The case of the Landers 1992 earthquake*

A preliminary study of the broadband records of the 1992 Landers earthquake seems to provide evidence for this frequency dependence of the directivity effect (Herrero, 1994). Figure 8 presents the ground acceleration spectra of 3 waveforms (AMB, PFO, and GSC) recorded at a similar distance from the fault (about 70 km) in three different directions. The strong motion record at AMB, at 90° from the rupture direction, can be used as a reference spectral shape. It does not significantly differ form the ω^2 model, with its flat acceleration

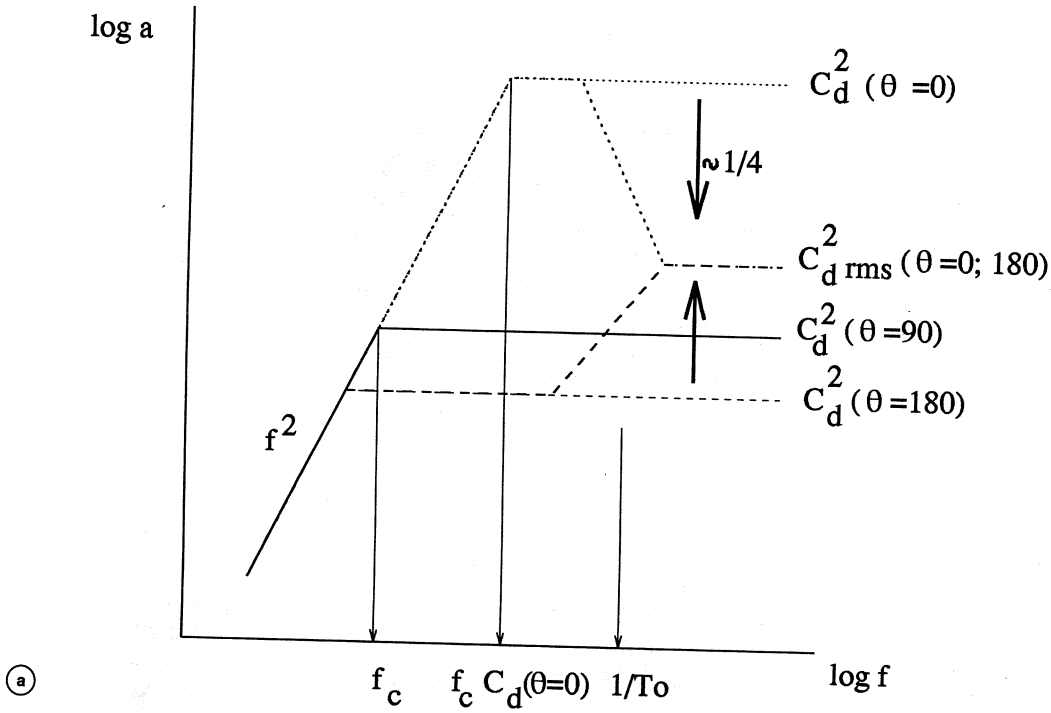

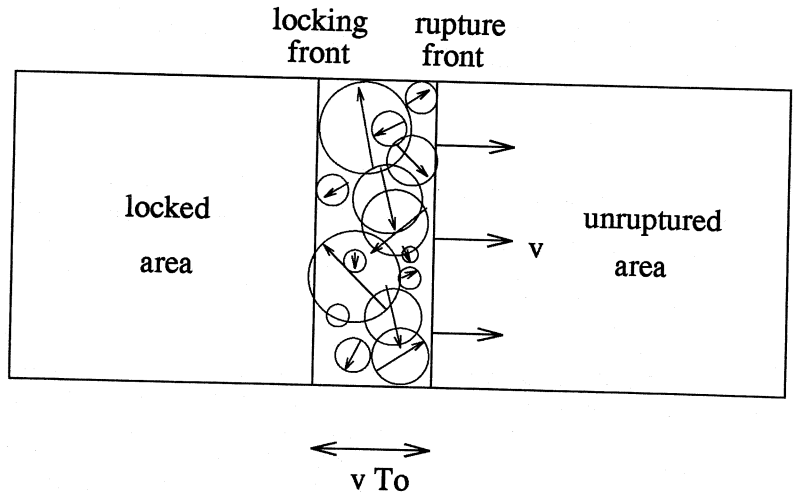

Fig. 7a,b. Frequency dependence of the directivity. The theoretical spectral levels $C_d^2(\theta = 0)$ and $C_d^2(\theta = 180°)$ deduced from our kinematic model for directive and anti-directive sites (a) may be significantly modified by some randomness of the subevents rupture direction in the slipping band (b). The $C_{d\,\mathrm{rms}}^2$ corresponds to a complete randomness for subevents sizes smaller than vT_0, which would affect the frequencies greater than about $1/T_0$.

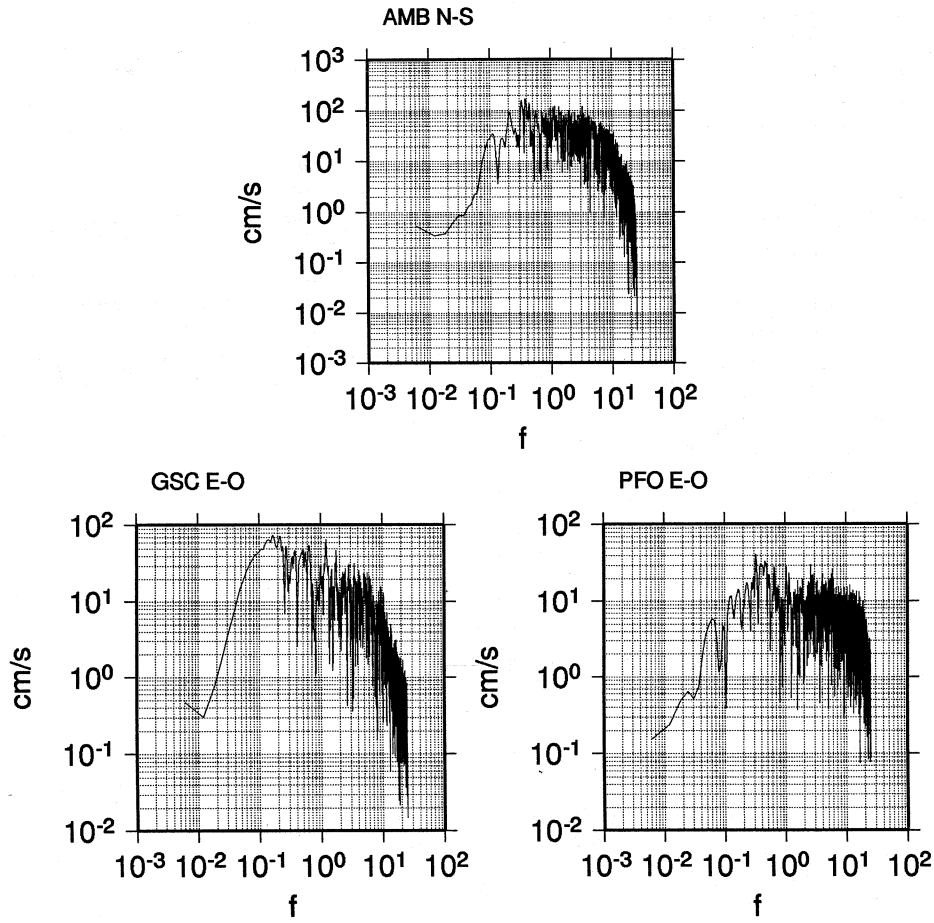

Fig. 8. Acceleration spectra for the Landers 1992 earthquake. Top: AMB (N-S); bottom left: GSC (E-W); bottom right: PFO (E-W). These stations are located at about 70 km from the center of the fault, in the direction of main rupture propagation (GSC: $\theta = 0°$), perpendicular to it (AMB: $\theta = 90°$), and opposite to it (PFO: $\theta = 180°$). The strong decay of the spectral acceleration level from intermediate to high frequencies at GSC is consistent with the frequency dependent model sketched in fig. 7a,b.

spectral level. The record at GSC, in the direction of the rupture, shows a clear decay of the spectral level going from the intermediate to the high frequencies. This cannot be an intrinsic source effect – such as a relatively large amplitude of the slip spectrum at intermediate wave numbers – as this does not appear at the two other sites.

We instead suggest that the distortion of the acceleration spectrum at GSC may be evidence for a frequency dependent directivity effect, which is predicted by our model as sketched in fig. 7. The transition frequency ranges approximately between 0.3 and 0.7 Hz. As the frequency at which the spectral level drops is $1/T_0$, the rise time T_0 ranges within 1.5 to 3.3 s. The corresponding length of the pulse thus ranges between 5 and 10 km. This is in agreement with recent results of waveform inversion for the Landers earthquake, which gave evi-

dence for the propagation of such a narrow pulse along the fault (Heaton, 1993; Cotton and Campillo, 1994). The record at PFO, opposite the direction of rupture, shows a clear depletion at the lowest frequencies, as expected.

7. Numerical kinematic model of complex rupture

From a numerical point of view, this frequency effect of the rupture directivity can be achieved by the following procedure (Herrero, 1994): the slip distribution is split into its high and low wave number components at the wave number $k = 1/vT_0$. The low wave number slip distribution is associated with a constant rupture velocity and an instantaneous slip, as before. The high wave-number slip presents areas of positive and negative slip on the fault plane, with complicated and variable shapes, which are considered independent subevents. These subevents break when one of their grid points (randomly chosen) is reached by the rupture front of the low wave number slip. A secondary «rupture» front then propagates in each of these subareas at a constant velocity. Because of the complicated shape of the subareas, and of the random nucleation point of the subevent, the rupture directions of the subevents are not specifically those of the main rupture, and the directivity effect is strongly reduced, as depicted in fig. 7a.

8. Conclusions

We propose a kinematic model based on a self-similar k^2 distribution of the coseismic slip, in order to distribute the sources of the high frequency radiation randomly on the fault plane. The slip instantaneously reaches its final value. At low wave number for the slip, the rupture front velocity is assumed to be constant, leading to an ω^2 body-wave radiation with a strong directivity effect around the corner frequency (factor C_d^2). At high wave number, the rupture is considered more stochastic, with independent subevents, reducing the directivity effect at high frequencies. Thus, paradoxically, this model predicts that the records at sites located in the direction of the rupture propagation are expected to be relatively enriched in low frequencies with respect to the high frequency level. The transition wavelength between the two processes may be related to the width of the actual slipping band, and the transition period in the radiated field to the actual rise-time.

Studies of ground motion spectral shapes at sites located in various azimuths with respect to the direction of rupture may thus provide a strong constraint on the average width of the propagating slip pulse, without the need for standard waveform inversion.

We therefore suggest that the spatial resolution for standard ground motion waveform inversion is limited by the length of the pulse: at lower wave numbers, the inversion is feasible, the «smoothed» rupture front presenting a regular shape, and the slip duration being approximately constant, proportional to the pulse length. At higher wave number, the speculated incoherence of the rupture drastically increases the number of free parameters to retrieve, although the number of available records is at most a few tens: the inversions are very likely to fail. Inversions of the higher frequencies of the records should therefore not consider the detailed phases of the seismogram, but only the amplitude spectra; accordingly, the resolved parameter on the fault plane would not be the slip history, but some radiation power distorted by some directivity coefficient.

This kinematic model can be used with more refined theoretical Green's functions, including near-field terms and surface waves, or with empirical Green's functions, for synthetizing realistic broadband strong ground motion (from 0 to about 20 Hz) in the vicinity of moderate to large earthquakes. These frequency and distance ranges are particularly relevant for engineering applications.

Acknowledgements

This work has been supported by INSU, France, and by the European EPOCH program, contract CT-91-0042.

REFERENCES

AKI, K. (1967): Scaling law of seismic spectrum, *J. Geophys. Res.*, **72**, 1217-1231.

ANDREWS, D.J. (1981): A stochastic fault model, 2. Time-dependent case, *J. Geophys. Res.*, **86**, 10821-10834.

BERNARD, P. (1987): Du caractere complexe et agressif des sources sismiques, *These de Doctorat d'Etat*, University of Paris 6, Paris.

BERNARD, P. and R. MADARIAGA (1984): A new asymptotic method for the modeling of near-field accelerograms, *Bull. Seismol. Soc. Am.*, **74**, 539-559.

BOATWRIGHT, J. and G.L. CHOY (1992): Acceleration source spectra anticipated for large earthquakes in Northeastern North America, *Bull. Seismol. soc. Am.*, **82**, 660-682.

BOORE, D.M. (1986): Short period *P* and *S*-wave radiation from large earthquake: implications for spectral scaling relations, *Bull. Seismol. Soc. Am.*, **76**, 43-64.

COTTON, F. and M. CAMPILLO (1994): Frequency domain inversion of strong motions: application to the 1992 Landers earthquake, *J. Geophys. Res.* (in press).

FRANKEL, A. (1991): High frequency spectral falloff of earthquakes, fractal dimension of complex rupture, *b* value, and the scaling of strength on fault, *J. Geophys. Res.*, **96**, 6291-6302.

HANKS, T.C. (1979): *b* values and ω^{γ} seismic source models: implications for tectonic stress variation along active crustal fault zones and the estimation of high frequency strong ground motion, *J. Geophys. Res.*, **84**, 2235-2242.

HARTZELL, S.H. and T.H. HEATON (1985): Teleseismic time functions for large, shallow subduction zone earthquakes, *Bull. Seismol. Soc. Am.*, **75**, 965-1004.

HEATON, T.H. (1990): Evidence for and implications of self-healing pulses of slip in earthquake rupture, *Phys. Earth Planet. Int.*, **64**, 1-20.

HEATON, T.H. (1993): Characteristics of the Landers earthquake rupture: implications for rupture physics, in *International School of Earth Geophysics, 9th Course: Earthquake Source Mechanics*, edited by ETTORE MAJORANA CENTER, Erice, 28-30.

HERRERO, A. (1994): Paramétrisation spatio-temporelle et spectrale des sources sismiques: application au risque sismique, *PhD. Thesis*, University of Paris 7, Paris.

HERRERO, A. and P. BERNARD (1994): A kinematic self-similar rupture process for earthquakes, *Bull. Seismol. Soc. Am.*, **84**, 1216-1228.

JOYNER, W.B. (1991): Directivity for non-uniform ruptures, *Bull. Seismol. Soc. Am.*, **81**, 1391-1395.

JOYNER, W.B. and D.M. BOORE (1981): Peak horizontal acceleration and velocity from strong ground motion records including records from the 1979 Imperial Valley California earthquake, *Bull. Seismol. Soc. Am.*, **71**, 2001-2038.

LOMNITZ-ADLER, J. and P. LEMUS-DIAZ (1989): A stochastic model for fracture growth on a heterogeneous seismic fault, *Geophys. J.*, **99**, 183-194.

PAPAGEORGIOU, A.S. and K. AKI (1983). A specific barrier model for the quantitative description of inhomogeneous faulting and the prediction of strong motion. Part I: Description of the model, *Bull. Seismol. Soc. Am.*, **73**, 693-722.